SCIENTIFIC REPORTS

OPEN

SUBJECT AREAS:
TWO-DIMENSIONAL MATERIALS
SPINTRONICS

Received
14 August 2013

Accepted
30 December 2013

Published
21 January 2014

Correspondence and requests for materials should be addressed to C.Z. (czhang@uow.edu.au)

Chiral-like tunneling of electrons in two-dimensional semiconductors with Rashba spin-orbit coupling

Yee Sin Ang[1], Zhongshui Ma[2,3] & C. Zhang[1,4]

[1]School of Physics, University of Wollongong, NSW 2522, Australia, [2]School of Physics, Peking University, Beijing 100871, China, [3]Collaborative Innovation Center of Quantum Matter, Beijing, 100871, China, [4]Institute for Superconducting and Electronic Materials, University of Wollongong, NSW 2522, Australia.

The unusual tunneling effects of massless chiral fermions (mCF) and massive chiral fermions (MCF) in a single layer graphene and bilayer graphene represent some of the most bizarre quantum transport phenomena in condensed matter system. Here we show that in a two-dimensional semiconductor with Rashba spin-orbit coupling (R2DEG), the real-spin chiral-like tunneling of electrons at normal incidence simultaneously exhibits features of mCF and MCF. The parabolic branch of opposite spin in R2DEG crosses at a Dirac-like point and has a band turning point. These features generate transport properties not found in usual two-dimensional electron gas. Albeit its π Berry phase, electron backscattering is present in R2DEG. An electron mimics mCF if its energy is in the vicinity of the subband crossing point or it mimics MCF if its energy is near the subband minima.

When a massless chiral fermion (mCF) encounters a potential barrier, reflection is completely suppressed due the forbidden spin-flipping transition, a phenomenon known as Klein tunneling[3]. The conservation of spin therefore leads to a perfect transmission of electrons through a high and wide potential barrier at normal incidence [Fig. 1(a)]. The 'Klein tunneling' was first described by Klein as a paradoxical behavior of relativistic electrons[3]. In single layer graphene (SLG), electrons in the vicinity of *K*-point follow linear energy dispersion and are chiral in the sense that the pseudospins, which represents the relative contribution from the sublattices, are locked to the direction of electron motion[1]. The low energy electrons in SLG are equivalent to a spin-1/2 mCF in relativistic quantum mechanics[2]. Due to the relativistic description of the Dirac quasiparticle, SLG serves as an ideal scaled-down platform to demonstrate the anomalous Klein tunneling in condensed matter systems[4–6]. In bilayer graphene (BLG), the low energy electrons mimic spin-1 massive chiral fermions (MCF). In contrast to SLG, electrons in BLG are reflected perfectly by a potential barrier at normal incidence [Fig. 1(a)]. Since such a perfect reflection of electrons is chiral in nature, it can be regarded as a 'Klein reflection' effect which has no counterpart in relativistic quantum mechanics.

So far the chiral tunneling in condensed matter systems is mostly focused on the pseudospin systems such as SLG, BLG and other graphene-related structures where electrons exhibit exotic and relativistic dynamics[7–11]. The exotic tunneling effects of massless chiral fermion and massive chiral fermions (MCF) are expected to be completely absent in non-relavistic Schrödinger systems. In this work, we shall demonstrate that the real-spin chiral-like tunneling in Schrödinger systems can exhibit both mCF-like and MCF-like tunneling behaviors. We consider a two dimensional semiconductor with Rashba spin-orbit coupling (R2DEG)[13–15] which is described by the following Hamiltonian,

$$H = \frac{p^2}{2m^*} + \frac{\lambda}{\hbar}(\sigma \times \mathbf{p})\cdot \mathrm{e}_z. \qquad (1)$$

Here σ is the Pauli spin matrix, λ is the Rashba spin-orbit coupling parameter and m^* is the electron effective mass. The eigenvalue is given as $E_s(k) = \hbar^2k^2/2m^* + s\lambda k$ ($s = \pm 1$). The band structure of R2DEG is shown in Fig. 1(b). The parabolic band of electrons with opposite spin are left-right shifted by $k_{SO} = m^*\lambda/\hbar^2$ in phase-space, giving rise to a subband crossing point (X-point) at $k = 0$. The energy difference between the X-point and the subband minima is given by $E_{SO} = m^*\lambda^2/2\hbar^2$. The chirality of the quasiparticle in SLG and BLG is loosely defined

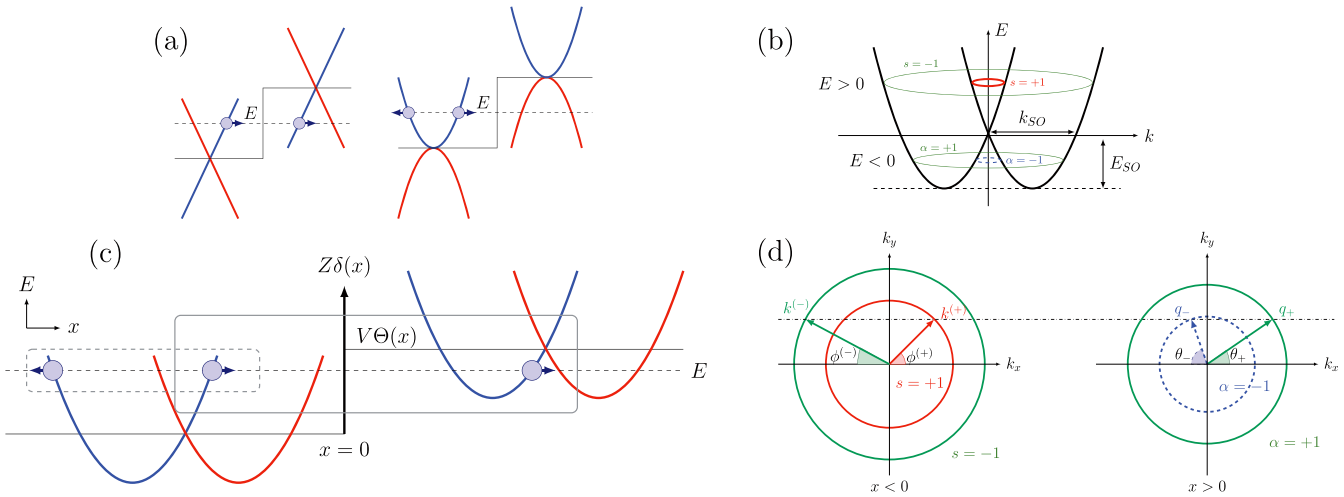

Figure 1 | Klein effect in condensed matter systems at normal incidence. (a) perfect transmission of massless chiral fermion in SLG and perfect reflection of massive chiral fermion in BLG. (b) Band structure of R2DEG. (c) Simultaneous mixture of massless and massive chiral fermions transport across a potential barrier $V(x)$ in R2EG. The tunneling process (outlined by solid box) mimics massless chiral fermion while the reflection process (outlined by dahsed box) mimics massive chiral fermion. In (a)–(c), the arrows denote the direction of motion of the quasiparticles and electrons. The blue and red branches denote the decoupled branches of opposite pseudospin [(a) and (b)] and real-spin [(c)] at normal incidence. (d) Fermi contours at the incident side ($x < 0$) and at the transmitted side ($x > 0$).

as the projection of the pseudospin on the particle's group velocity[4,12], i.e. $\hat{v}\cdot\hat{\sigma}$, where $\hat{v}$ and $\hat{\sigma}$ are the unit vectors of the group velocity and pseudospin respectively. In R2DEG, the spin polarization lies in the plane of the electron gas and is perpendicular to the electron wavevector. It is not possible to define 'chirality' using the same dot product method. However, all electrons residing in a particular Fermi circle do follow a fixed $\hat{v}\times\hat{P}$ relation where $\hat{P}$ is the direction of real-spin and hence the electrons can be regarded as 'chiral-like'. Such a description allows us to link the real-spin chiral-like tunneling phenomena in R2DEG directly with the pseudospin chiral tunneling effect in SLG and BLG. Furthermore, the two branches of opposite pseudospins cross and touch in SLG and BLG respectively. The crossing and touching points are commonly known as the 'Dirac point' due to the relativistic dynamics of the quasiparticles. In R2DEG, the spin splitting, and hence the formation of the X-point, has its root from the relativistic effect of the electrically confined electrons (which manifests itself as a Rashba Hamiltonian linear in k). This justifies the interpretation of the electron tunneling across the Dirac-like X-point in R2DEG as a chiral-like tunneling phenomenon.

The energy dispersion of electrons at the vicinity of the X-point is nearly linear and therefore closely resembles the mCF dispersion in SLG. Additionally, electrons at the vicinity of the subband minima are furthest away from the linear X-point and exhibits the strongest parabolicity. As a result, these electrons mimic the MCF in BLG. As shown in Fig. 1(c), an incident electron can only be scattered by a potential barrier to states lying in the same spin-split subband in order to conserve real-spin. For transport of an electron of a given energy with respect to the X-point, two possibilities arise: (1) electron transmission to a spin non-flipping state below the X-point or (2) electron reflection to a spin non-flipping state above the X-point. Process (1) is in the same spirit as the Klein tunneling of mCF in SLG while process (2) is more akin to the Klein reflection of MCF in BLG. The electron quantum transport across a potential barrier in R2DEG can thus exhibit both mCF-like and MCF-like behaviors.

Results

Transmission and reflection probabilities. The electron transport across a potential barrier $V(x)$ in R2DEG is governed by the Hamiltonian,

$$H(x,k)=\begin{pmatrix}\frac{\hbar^2k^2}{2m^*}+V(x) & \lambda(k_y+ik_x)\\ \lambda(k_y-ik_x) & \frac{\hbar^2k^2}{2m^*}+V(x)\end{pmatrix}. \qquad (2)$$

We model the potential barrier by $V(x) = \Theta(x)V_0 + \delta(x)Z$, where $\Theta(x)$ is a Heaviside step function, $\delta(x)$ is a Dirac delta function, V_0 and Z denotes the height of the step potential and the strength of an interface potential respectively [Fig. 1(c)]. In order to make parallel comparison with the chiral tunneling of electrons in SLG and BLG, we consider only the case where the incident state lies above the X-point with $E > 0$ and the transmitted state lies below the X-point with $E < 0$. This sets up an incident energy condition of $V_0 > E > V_0 - E_{SO}$. For electrons incident from the left of the junction ($x < 0$), an $E > 0$ constant energy surface intersects both $s = \pm 1$ branches at two concentric circles of radius $k^{(s)}=\sqrt{2m/\hbar^2(E_{SO}+E)}-sk_{SO}$. For the transmitted electron in the region of $x > 0$, an $E < 0$ constant energy surface intersects only the $s = -1$ branch. However, due to the existence of a subband turning point (i.e. the subband minimum), the constant energy surface again intersects two concentric circles of radius $q_\alpha=k_{SO}+\alpha\sqrt{2m/\hbar^2(E_{SO}+E-V)}$ where $\alpha = \pm 1$ [Fig. 1(d)]. Unlike SLG and BLG where $s = -1$ states are always hole-like in the sense that the motion of electron is antiparallel to its wavevector, the $s = -1$ branch states of R2DEG are electron-like in the outer circle $\alpha = +1$ and hole-like in the inner circle $\alpha = -1$. The existence of hole-like states in the $s = -1$ branch suggests that negative electron refraction and electron focusing effect[16,17], previously reported in SLG[11], BLG[18] and topological insulator[19,20], can also be realized in R2DEG via transmission of electrons to $\alpha = -1$ circle of the $s = -1$ branch.

The eigenstates of Eq. (1) for electrons in the $x < 0$ and the $x > 0$ region are given as $\xi^{(s)}=1/\sqrt{2}\left(1,-sie^{i\phi^{(s)}}\right)^T$ and $\xi_\alpha^{(-)}=1/\sqrt{2}\left(1,ie^{i\theta_\alpha}\right)^T$, respectively. Generally, an electron in s-state incident from the $x < 0$ region can be reflected to s and $-s$ branches in the region $x < 0$, or be transmitted to $\alpha = \pm 1$ states in the region of $x > 0$. The reflected and transmitted angles, ϕ's and θ's, are related by the conservation of momentum component parallel to the interface, i.e.

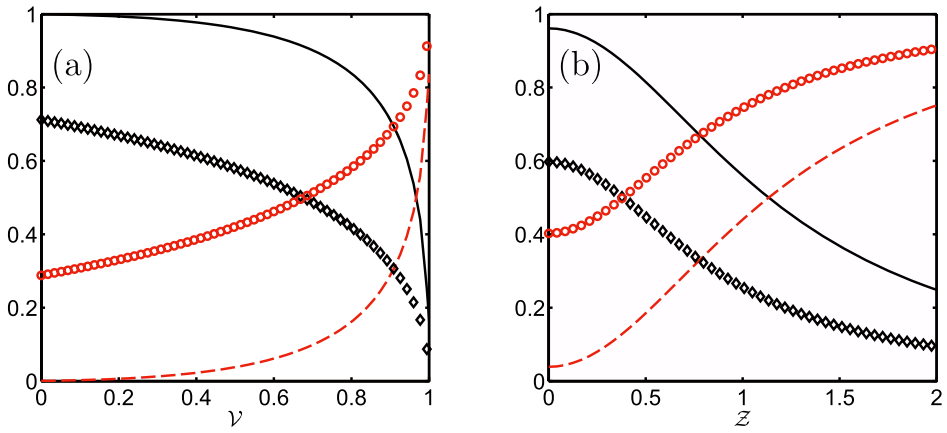

Figure 2 | Transmission/reflection probabilites at normal incidence, (a) at different $\mathcal{V}$ with $\mathcal{Z}=0$, solid line: $T^{(s)}_{\bar{s}}(\mathcal{E}=0.1)$, dashed line: $R^{(s)}_{\bar{s}}(\mathcal{E}=0.1)$, ○: $T^{(s)}_{\bar{s}}(\mathcal{E}=10)$, ◇: $R^{(s)}_{\bar{s}}(\mathcal{E}=10)$; and (b) at different $\mathcal{Z}$ with $\mathcal{E}=1$, solid line: $T^{(s)}_{\bar{s}}(\mathcal{V}=0.1)$, dashed line: $R^{(s)}_{\bar{s}}(\mathcal{V}=0.1)$, ○: $T^{(s)}_{\bar{s}}(\mathcal{V}=0.9)$, ◇: $R^{(s)}_{\bar{s}}(\mathcal{V}=0.9)$.

$k^{(s)}\sin\phi^{(s)}=k^{(-s)}\sin\phi^{(-s)}=q_\alpha\sin\theta^{(-)}_\alpha$ where $k^{(s)}$ and $\phi^{(s)}$ are the magnitude and direction of the incident wavevector. We construct the total wavefunctions in the $x<0$ region Ψ_L and in the $x>0$ region Ψ_R. The transmission/reflection probabilities can be obtained by connecting Ψ_L and Ψ_R via the boundary conditions $\Psi_L|_{x=0}=\Psi_R|_{x=0}$ and $\Psi'_R|_{x=0}-\Psi'_L|_{x=0}=(2mZ/\hbar^2)\Psi_R|_{x=0}$. At normal incidence, the probabilities are found as,

$$\begin{aligned}
R^{(s)}_{s}\left(\phi^{(s)}=0\right)&=T^{(s)}_{\alpha=s}\left(\phi^{(s)}=0\right)=0,\\
R^{(s)}_{-s}\left(\phi^{(s)}=0\right)&=\frac{\left(\sqrt{1+\mathcal{E}}-\sqrt{1-\mathcal{V}}\right)^2+4\mathcal{Z}^2}{\left(\sqrt{1+\mathcal{E}}+\sqrt{1-\mathcal{V}}\right)^2+4\mathcal{Z}^2},\\
T^{(s)}_{\alpha=-s}\left(\phi^{(s)}=0\right)&=\frac{4\sqrt{1+\mathcal{E}}\sqrt{1-\mathcal{V}}}{\left(\sqrt{1+\mathcal{E}}+\sqrt{1-\mathcal{V}}\right)^2+4\mathcal{Z}^2},
\end{aligned}\tag{3}$$

where we have defined dimensionless parameters $\mathcal{E}=E/E_{SO}$, $\mathcal{V}=(V-E)/E_{SO}$ and $\mathcal{Z}=Z/\lambda$. $R^{(s)}_{s'}$ denotes the reflection probability of $s\rightarrow s'$ reflection process and $T^{(s)}_{\alpha}$ denotes the transmission of an s incident state into an α state of $s=-1$ branch. The spinors are states of a spin component orthogonal to $\mathbf{k}$ so that the spin orientation always points in a direction perpendicular to $\mathbf{k}$. At normal incidence, $R^{(s)}_{s}$ and $T^{(s)}_{\alpha=s}$ are strictly zero since the cross-subband processes of $s\rightarrow s$ reflection and s to $\alpha=s$ transmission requires reversal of spin orientation. Therefore only the spin non-flipping transitions of $s\rightarrow -s$ reflection and $\alpha=-s$ transmission are permissible, leading to non-zero $R^{(s)}_{-s}$ and $T^{(s)}_{-s}$ at normal incidence.

Eq. (3) reveals that the two parabolic branches of opposite spin are decoupled. Such decoupling is also evident in SLG and BLG at normal incidence. In fact, the decoupling of branches of opposite pseudospin is the most important condition for the Klein tunneling and the Klein reflection. In SLG, the mCF energy spectrum decouples into two independent linear branches of opposite pseudospin crosses at the Dirac point whereas in BLG, the MCF energy spectrum decouples into two independent parabolic branches touching at the Dirac point. Due to this decoupling, the mCF must be confined in its own pseudospin branch, leading to the Klein tunneling of mCF across a potential barrier. In BLG, the decoupled pseudospin branch only touches at the Dirac point without any band crossing. Since there is a band turning in the parabolic pseudospin branch, the confinement of electron within a decoupled pseudospin branch requires to electron to be reflected. In R2DEG, the decoupled real-spin branches are parabolic and has a band turning point (as in the case of BLG), and they also cross each other at the X-point (as in the case of SLG). The electron transport is therefore a hybrid of the tunneling phenomena in SLG and BLG. In Eq. (3), it is seen that the transmission and reflection within the same real-spin branches are both finite. This further elucidates the hybrid between of mCF and MCF behaviours in R2DEG.

Whether an incident electron is preferentially transmitted or reflected depends on the properties of the incident and transmitted states in the R2DEG band structure and is influenced by $\mathcal{E}$ and $\mathcal{V}$. The energy parameter $\mathcal{E}$ characterizes the 'Dirac-ness' of the incident electron, with $\mathcal{E}\rightarrow 0$ representing a mCF-like incident state at the vicinity of the X-point. The potential parameter $\mathcal{V}$, ranging from 0 to 1, characterizes the 'Dirac-ness' of the transmitted electron. In the trivial case when $\mathcal{V}\rightarrow 0$, the transmitted state is at the vicinity of the X-point and the electrons mimic mCF in SLG. In contrast to $\mathcal{V}\rightarrow 0$, when $\mathcal{V}\rightarrow 1$, the transmitted state is at the vicinity of the subband minima and the electrons are MCF-like, as in the case of BLG. In Fig. 2(a), we show the crossover of the transmission/reflection probabilities from mCF-like behavior to the MCF-like behavior when $\mathcal{V}$ varies from 0 to 1 with $\mathcal{Z}=0$. We first restrict ourselves to the extreme case of Dirac-like incident state at an energy $\mathcal{E}=0.1$ with (i) $\mathcal{V}\rightarrow 0$ and (ii) $\mathcal{V}\rightarrow 1$. Case(i) is the trivial case where the mismatch between the incident and the transmitted states is vanishingly small. In this case, electron transport occurs around the X-point and is dominated by very high transmission. For case (ii), the transmitted state is further away from the X-point and is MCF-like. We obtain a completely opposite result where electrons are reflected with high probability. Therefore, the highly transmitting mCF-like behavior and the highly reflective MCF-like behavior are both present in R2DEG. At intermediate $\mathcal{E}$ and $\mathcal{V}$, the quantum transport phenomena is a mixture of the mCF and MCF tunneling effects where both transmission and reflection are possible. We emphasize that the electron transport in R2DEG is a hybrid of transmission of the mCF and reflection of the MCF. Perfect Klein tunneling and Klein reflection of electrons does not occur in R2DEG unless in the above mentioned trivial cases.

When $\mathcal{V}\rightarrow 1$, reflection dominates because of the vanishing Fermi radius of the transmitted states. We would like to point out an interesting situation when $\mathcal{E}\rightarrow 0$ and $\mathcal{V}\rightarrow 1$. The incident electron is mCF-like while the transmitted state is at the proximity of the subband minima and is MCF-like. The 'massless' incident state prefers transmission while the 'massive' transmitted state forbids transmission. This is loosely analogous to the situation of 'an unstoppable object meeting an impenetrable barrier'. In fact, the chiral tunneling of electron at normal incidence can be interpreted as the absence of the $s\rightarrow s$ reflection process due to the spin non-flipping requirement. In graphene, there is only one possible pseudospin non-flipping

transmission mode while in R2DEG there exists an additional spin non-flipping reflection state in the $s = -s$ branch. The electron transport condition can be re-stated as: (i) no $s \rightarrow s$ reflection as required by the incident state; and (ii) no $\alpha = -s$ transmission as required by the transmitted state. This leaves the incident electron with only one choice, i.e. to be reflected to the $-s$ branch. In Fig. 3(b), we show the transmission/reflection probabilities in the presence of an interface potential $\mathcal{Z} > 0$. Reflection of $s \rightarrow s$ and transmission to $\alpha = -s$ are always forbidden regardless the strength of $\mathcal{Z}$. The interface potential in the present structure is non-magnetic and the spin-orbit coupling is not due to spin accumulation. As a result the chiral tunneling in R2DEG is well protected from the interface potential. The effect of $\mathcal{Z}$ is to enhance the $R^{(s)}_{-s}$ reflection and to suppress the $T^{(s)}_{-s}$ transmission (shown in Fig. 2(b)). In the extreme case of $\mathcal{Z} \rightarrow \infty$, it can be shown from Eq. (2) that $R^{(s)}_{-s} = 1$ and $T^{(s)}_{-s} = 0$.

Berry phase and electron backscattering. When electrons are transported around a closed loop adiabatically in k-space, the wavefunction acquires an additional Berry phase of geometric nature: $\gamma = \oint_c d\mathbf{k} \cdot \mathcal{A}$, where the Berry connection is $\mathcal{A} = i\xi^{\dagger}_s(\mathbf{k})\nabla_{\mathbf{k}}\xi_s(\mathbf{k})$[21]. The Berry phase is closely related to the transport phenomena. One classic example being graphene where the π Berry phase associated with the pseudospin rotation leads to the absence of electron backscattering[22,23]. In R2DEG, $\mathcal{A} = -1$ and the Berry phase is also π[24]. Electron backscattering is, however, permissible in R2DEG. To illustrate this peculiar result, we consider the spin polarization: $\mathrm{P}_s = \xi^{\dagger}_s \sigma \xi_s$. Because $\mathbf{P}_s \cdot (\mathbf{k}/k) = 0$, the spin is perpendicular to the electron wavevector $\mathbf{k}$. Furthermore, spin polarization is contained entirely in the plane of the R2DEG and it rotates, with respect to $\mathbf{k}$, in opposite directions along the $s = \pm 1$ Fermi circles ($\mathbf{P}_s$ rotates in clockwise direction along the $s = +1$ Fermi circle and in anti-clockwise direction along the $s = -1$ Fermi circle) as dictated by $\mathrm{P}_s \times (\mathrm{k}/k) = s\hat{z}$. For an incident electron with incident angle $\phi^{(s)}$, the spin polarization is $\mathrm{P}^{(i)}_s = s\left(\hat{\mathrm{x}}\sin\phi^{(s)} - \hat{\mathrm{y}}\cos\phi^{(s)}\right)$. The reflected electron spin polarization is

$$\mathrm{P}^{(r)}_{\pm s} = \pm s\left(\hat{\mathrm{x}}\sin\phi^{(s)} + \hat{\mathrm{y}}\cos\phi^{(s)}\right), \tag{4}$$

for $s \rightarrow s$ and $s \rightarrow -s$ reflection respectively. At normal incidence, the spin polarizations of both incident and reflected electrons are purely y-directional: $\mathrm{P}^{(i)}_s = -s\hat{\mathrm{y}}$ and $\mathrm{P}^{(r)}_{\pm s} = \pm s\hat{\mathrm{y}}$. Correspondingly, $\mathrm{P}^{(i)}_s = \mp \mathrm{P}^{(r)}_{\pm s}$ and this implies that the spin orientation is reversed in $s \rightarrow s$ reflection while it remains unchanged in $s \rightarrow -s$ reflection. During the spin-flipping $s \rightarrow s$ reflection, electron acquires an additional π Berry phase and, as in the case of the psudospin chiral tunneling in graphene, $s \rightarrow s$ backscattering is forbidden. However, in the spin non-flipping $s \rightarrow -s$ reflection process, the electron does not acquire an additional Berry phase. Consequently, the $s \rightarrow -s$ backscattering is permissible and this leads to the rather surprising result that electron backscattering is *present* in R2DEG albeit its π Berry phase.

Spin-polarized transmission through a *n-p* junction. The numerical results for finite incident angle transmission/reflection probabilities are shown in Fig. 3 for two incident states $s = \pm 1$ with $\mathcal{E} = 1$ and $\mathcal{V} = 0.5$. At finite incident angles, $R^{(s)}_s$ and $T^{(s)}_s$ are no longer zero since the spins are mixed. The transmission and reflection probabilities sum up to one as there is only one incident electron and the electron current moving across the interface is conserved as

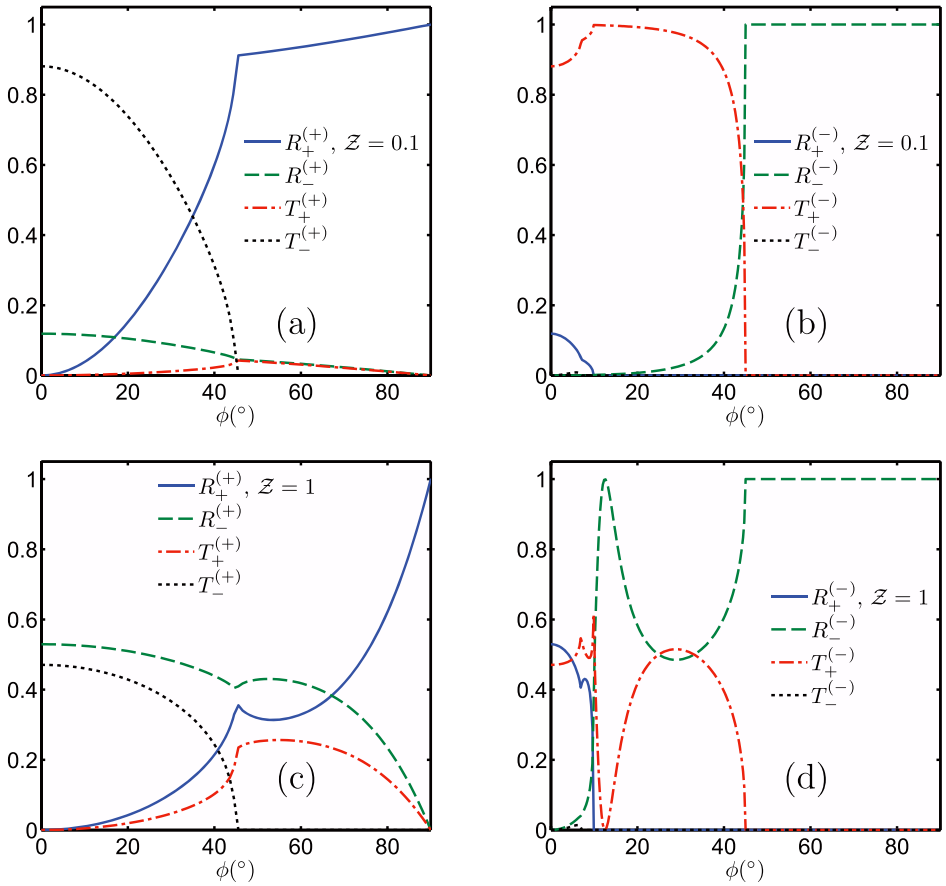

Figure 3 | Probabilities at finite incident angle ϕ at two incident states $s = \pm 1$ with $\mathcal{Z} = 0.1$ in (a) and (b); and with $\mathcal{Z} = 1$ in (c) and (d).

required by the charge continuity condition. For the $s=-1$ to $s=1$ reflection process, there exists a critical incident angle of $\phi^{(-),c}=\sin^{-1}(k^{(+)}/k^{(-)})$. The critical angle for the transmission of s incident state is given as $\phi_{\alpha}^{(s),c}=\sin^{-1}\left(q_{\alpha}\Big/k^{(s)}\right)$. The transmission/reflection probabilities vanishes when the critical incident angle is exceeded. In Fig. 3(a), $T_{-}^{(-)}$ dominates when the incident angle is small. For incident angle greater than $\phi_{-}^{(+),c}$, $T_{+}^{(+)}$ becomes the only permissible transmission process. For the $s=-1$ incident state, the $\alpha=-1$ branch has a relatively small radius in k-space. Due to the smallness of $\phi_{-}^{(-),c}$, the $T_{-}^{(-)}$ process is nearly absent as shown in Fig. 3(b). For small and intermediate incident angles, the $s=-1$ incident electron prefers $R_{+}^{(-)}$ reflection and $T_{+}^{(-)}$ tunneling where the mismatch of spin orientation is not too large. Once the incident angle exceeds $\phi^{(-),c}$, $T_{+}^{(-)}$ tunneling becomes the only possible process and hence $T_{+}^{(-)}\approx 1$ up to the intermediate incident angle regime. At larger incident angle, the mismatch of spin polarization of the $R_{-}^{(-)}$ reflection decreases and $R_{-}^{(-)}$ rapidly approaches unity. The effects of the interface potential $\mathcal{Z}$ on the transmission/reflection probabilities are shown in Fig. 3(c) and 3(d). For the $s=+1$ incident state, $\mathcal{Z}$ suppresses transmission and amplifies reflection at small incident angle. At larger incident angle, $\mathcal{Z}$ however promotes the transmission to $\alpha=+1$ [Fig. 3(c)]. For the $s=-1$ incident state, transmission is always suppressed. Interestingly, $R_{+}^{(-)}$ is briefly unity well before the termination of $T_{+}^{(-)}$ [Fig. 3(d)]. Since the electron transport across a potential barrier in R2DEG is sensitively influenced by $\mathcal{E}$, $\mathcal{V}$ and $\mathcal{Z}$, tuning of these parameters offers a possibility of manipulating the spin polarization of the transmitted electrons. We further investigate the spin-polarized electron transport by defining

$$\Delta\mathcal{T}(\mathcal{E},\mathcal{V})=\sum_{s}\int_{0}^{\frac{\pi}{2}}\left(\frac{T_{+}^{(s)}(\phi,\mathcal{E},\mathcal{V})-T_{-}^{(s)}(\phi,\mathcal{E},\mathcal{V})}{T_{+}^{(s)}(\phi,\mathcal{E},\mathcal{V})+T_{-}^{(s)}(\phi,\mathcal{E},\mathcal{V})}\right)\mathrm{d}\phi. \qquad (5)$$

Here, $\Delta\mathcal{T}>0(\Delta\mathcal{T}<0)$ represents the excess transmission of electrons to $\alpha=+1$ ($\alpha=-1$) branch. In Fig. 4(a), $\Delta\mathcal{T}$ is dominantly positive when $\mathcal{V}\to 0$ due to the smallness of the critical angles of $T_{-}^{(\pm)}$. $\Delta\mathcal{T}$ is dominantly negative when $\mathcal{V}\to 1$ where the radius of the $\alpha=-1$ branch in phase-space is large enough to accommodate more electron transmissions. In general, $\mathcal{Z}$ does not significantly modify $\Delta\mathcal{T}$ with the exception that at large $\mathcal{V}$, transmission to the $\alpha=-1$ state is strongly enhanced by small $\mathcal{Z}\approx 0.2$ as shown in Fig. 4(b). Fig. 4(a) and Fig. 4(b) suggest that $\mathcal{V}$ plays an important role in determining the sign of $\Delta\mathcal{T}$. We verified this by examining the $\mathcal{Z}$-and $\mathcal{E}$-dependence of $\Delta\mathcal{T}$ at two contrasting choices of $\mathcal{V}=0.1$ in Fig. 4(c) and $\mathcal{V}=0.9$ in Fig. 4(d). At $\mathcal{V}=0.1$, $\Delta\mathcal{T}>0$ in the entire ranges of $0<\mathcal{E}<2$ and $0<\mathcal{Z}<5$ [Fig. 4(c)]. The

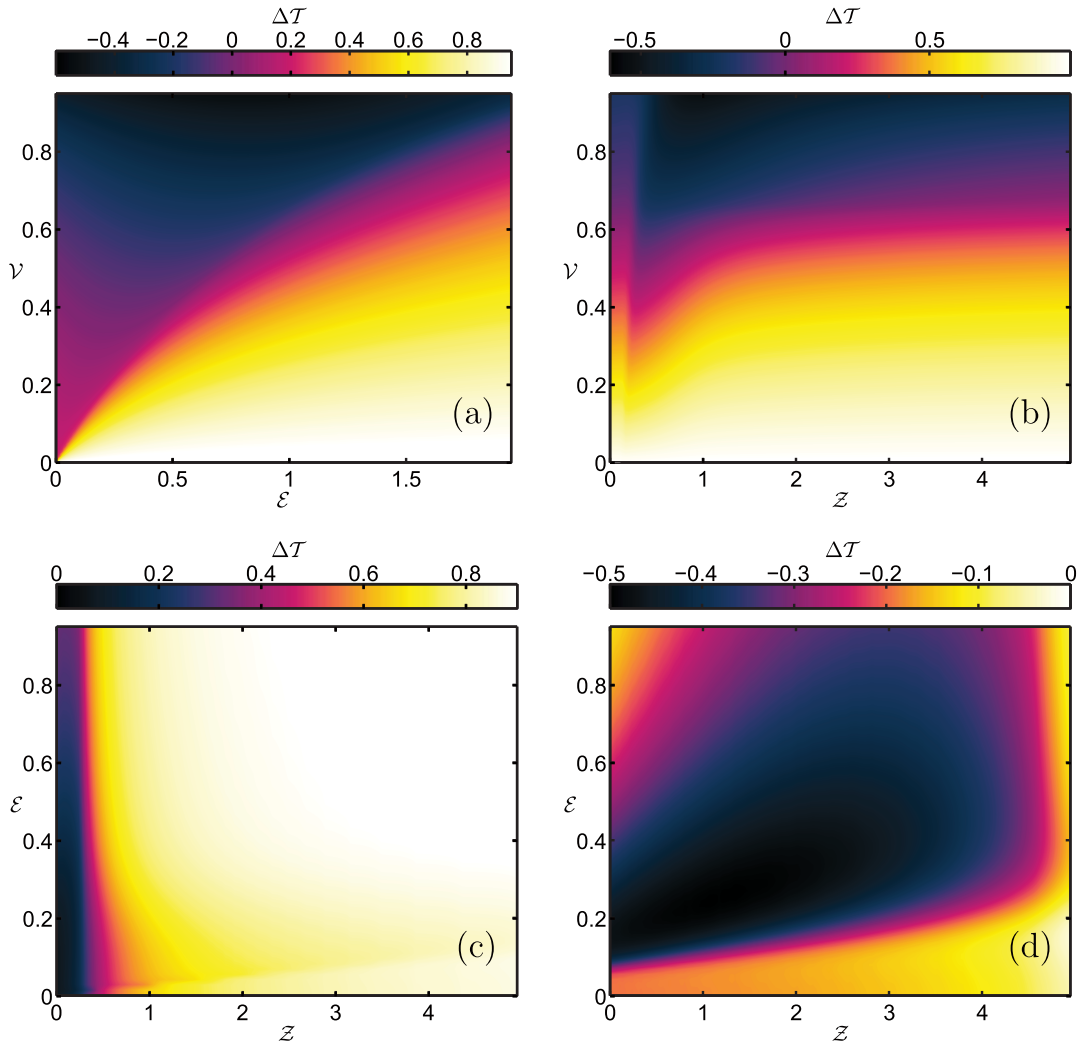

Figure 4 | Dependence of spin-polarization, $\Delta\mathcal{T}$, on $\mathcal{V}$, $\mathcal{E}$ and $\mathcal{Z}$. (a) $\mathcal{V}$-and $\mathcal{E}$-dependence at $\mathcal{Z}=1$. (b) $\mathcal{V}$-and $\mathcal{Z}$-dependence at $\mathcal{E}=1$. $\mathcal{E}$-and $\mathcal{Z}$-dependence at (c) $\mathcal{V}=0.1$; and (d) $\mathcal{V}=0.9$.

polarization is completely reversed to $\Delta\mathcal{T} < 0$ at $\mathcal{V} = 0.9$ as shown in Fig. 4(d). This immediately suggests that electrons are preferably transmitted to $\alpha = +1$ ($\alpha = -1$) branch if the transmission state mimics massless (massive) chiral fermion. The R2DEG junction thus works as a spin-polarizer which polarizes electrons into $\alpha = \pm 1$ branches depending on the choice of $\mathcal{V}$.

Discussion

We have calculated the electron transport across a step potential in R2DEG. We demonstrated the simultaneous occurrence of both mCF- and MCF-like tunneling behavior in a non-relativistic Schrödinger system. The Rashba spin-orbit coupling can give rise to adjustable transparency for electron transport at a semiconductor junction. Apart from the non-relativistic nature of the R2DEG system, there is another interesting distinction between the chiral tunneling in the present system and the chiral tunneling in a relativistic system or in SLG. In graphene, incident electrons are in the conduction band and transmitted electrons are in the valence band. In the present system, the states on the two sides of the junction are both in the conduction band and the valence band is not involved in our analysis. The results presented in this work is in the ballistic transport regime where the sample size is assumed to be smaller than the electron mean free path. In the diffusive regime where disorder and interaction is important, localization of the two-dimensional electron gas is expected to occur[25,26]. Weak localization of electrons in R2DEG has been experimentally observed in a Zn doped p-type InAs single crystal[27]. We therefore expect our results to be quantitatively different with that of the diffusive regime. However, as long as the impurity does not cause spin-flipping, the chiral-like transport phenomena at normal incidence will remain valid. To observe the R2DEG electron transport and its crossover between mCF and MCF behavior, a large E_{SO} is preferred since it allows a larger tuning range for $\mathcal{V}$. Experimental results on layered semiconductor BiTeI[28] and surface state of Bi/Ag(111)[29] have revealed giant RSOI with E_{SO} in the order of 10^2 meV. A junction based on these materials may be a suitable system to experimentally study the the crossover from mCF-like and MCF-like tunneling phenomena.

Methods

In this section, we briefly discuss the general procedures to obtain the transmission and reflection probabilities. On the incident side ($x < 0$), the total wavefunction is given as

$$\Psi_L = \xi^{(s)} e^{ik^{(s)}\cos\phi^{(s)}x} + \sum_{s'=\pm 1} r_{s'}^{(s)} \xi^{(s')*} e^{-ik^{(s')}\cos\phi^{(s')}x} \tag{6}$$

where $s = \pm 1$, $*$ denotes complex conjugate, $\phi^{(s)}$ is the angle of incidence of an electron in the s-branch and $r_{s'}^{(s)}$ denotes the reflection coefficients of the $s \to s'$ reflection process. The eigenstate can be explicitly written as

$$\xi^{(s)} = \begin{bmatrix} 1 \\ -ise^{-i\phi^{(s)}} \end{bmatrix} \tag{7}$$

On the transmitted side ($x > 0$), the total wavefunction is given as

$$\Psi_R = t_+^{(s)} \xi_+ e^{iq_+\cos\theta_+ x} + t_-^{(s)} \xi_-^* e^{-iq_-\cos\theta_- x} \tag{8}$$

where $t_\pm^{(s)}$ is the transmission coefficients to $\alpha = \pm 1$ state. The second term of Eq. (8) is a hole-like transmitted state whose direction of motion is antiparallel with its wavevector and hence it carries a factor of $e^{-iq_-\cos\theta_- x}$. The eigenstate is given as

$$\xi_\pm = \begin{bmatrix} 1 \\ \mp ise^{\pm i\theta_\alpha} \end{bmatrix} \tag{9}$$

Due to the conservation of k_y, the $s \to s'$ reflection angles can be obtained vas $\phi^{(s')} = \sin^{-1}(k^{(s)}/k^{(s')}\sin\phi^{(s)})$ and the transmission angles into the α branch can be obtained as $\theta_\alpha = \sin^{-1}(k^{(s)}/q_\alpha \sin\phi^{(s)})$, where $\phi^{(s)}$ and $k^{(s)}$ are the incident angle and wavevector respectively and $s' = \pm 1$. Ψ_L and Ψ_R can be connected by the boundary conditions at $x = 0$, i.e. $\Psi_L|_{x=0} = \Psi_R|_{x=0}$ and $d_x\Psi_R|_{x=0} - d_x\Psi_L|_{x=0} = 2mZ/\hbar^2$. This leads to a set of simultaneous equations

$$\begin{pmatrix} 1 & 1 & -1 & -1 \\ e^{i\phi(+)} & -e^{i\phi(-)} & -e^{i\theta_+} & e^{-i\theta_-} \\ -k^{(+)}\cos\phi^{(+)} & -k^{(-)}\cos\phi^{(-)} & -Q_+ & Q_- \\ k^{(+)}\cos\phi^{(+)}e^{i\phi(+)} & -k^{(-)}\cos\phi^{(-)}e^{i\phi(-)} & Q_+e^{i\theta_+} & Q_-e^{-i\theta_-} \end{pmatrix} \begin{pmatrix} r_+^{(s)} \\ r_-^{(s)} \\ t_+^{(s)} \\ t_-^{(s)} \end{pmatrix} = \begin{pmatrix} -1 \\ se^{i\phi^{(s)}} \\ -k^{(s)}\cos\phi^{(s)} \\ -sk^{(s)}\cos\phi^{(s)}e^{i\phi^{(s)}} \end{pmatrix} \tag{10}$$

where $Q_\pm = q_\pm\cos\theta_\pm \pm i2mZ/\hbar^2$. The transmission and reflection coefficients can then be solved and the probabilities are determined from

$$\begin{aligned} R_{s'}^{(s)} &= \frac{v_{s'}}{v_s}\left|r_\pm^{(s)}\right|^2 \\ T_\alpha^{(s)} &= \frac{\mu_\alpha}{v_s}\left|r_\pm^{(s)}\right|^2 \end{aligned} \tag{11}$$

where $s = \pm 1$ and $s' = \pm 1$. v_s, $v_{s'}$ and $u_\pm$ are the x-directional component of the incident and reflected electron group velocity at $x < 0$ and of the transmitted electron group velocity for $x > 0$ respectively. These are given by,

$$\begin{aligned} v_s &= \sqrt{\tfrac{2}{m^*}(E_{SO}+E)}\cos\phi^{(s)} \\ v_{s'} &= \sqrt{\tfrac{2}{m^*}(E_{SO}+E)}\cos\phi^{(s')} \\ \mu_\alpha &= \sqrt{\tfrac{2}{m^*}(E_{SO}+E-V)}\cos\theta_\alpha \end{aligned} \tag{12}$$

At normal incidence, Eq. (10) reduces to

$$\begin{pmatrix} 1 & 1 & -1 & -1 \\ 1 & -1 & -1 & 1 \\ -k^{(+)} & -k^{(-)} & -Q'_+ & Q'_- \\ k^{(+)} & -k^{(-)} & Q'_+ & Q'_- \end{pmatrix} \begin{pmatrix} r_+^{(s)} \\ r_-^{(s)} \\ t_+^{(s)} \\ t_-^{(s)} \end{pmatrix} = \begin{pmatrix} -1 \\ s \\ -k^{(s)} \\ -sk^{(s)} \end{pmatrix} \tag{13}$$

where $Q'_\pm = q_\pm \pm i2mZ/\hbar^2$. Eq. (13) can be decoupled into two sets of equations:

$$\begin{cases} r_+^{(s)} - t_+^{(s)} = \frac{s-1}{2} \\ k^{(+)}r_+^{(s)} + Q'_+ t_+^{(s)} = \frac{1-s}{2}k^{(s)} \end{cases} \tag{14}$$

$$\begin{cases} r_-^{(s)} - t_-^{(s)} = \frac{-1-s}{2} \\ k^{(+)}r_-^{(s)} + Q'_+ t_-^{(s)} = \frac{-1-s}{2}k^{(s)} \end{cases} \tag{15}$$

Solving the above equation, we obtain

$$\begin{aligned} r_s^{(s)} &= t_s^{(s)} = 0 \\ r_{-s}^{(s)} &= \frac{k^{(s)} + sQ'_{-s}}{k^{(-s)} - sQ'_{-s}} \\ t_{-s}^{(s)} &= \frac{k^{(+)} + k^{(-)}}{k^{(-s)} - sQ'_{-s}} \end{aligned} \tag{16}$$

Knowing that the wavevectors are related by $k^{(s)}\sin\phi^{(s)} = k^{(-s)}\sin\phi^{(-s)} = q_\alpha \sin\theta_\alpha^{(-)}$ and defining $\mathcal{E} = E/E_{SO}$, $\mathcal{V} = (V-E)/E_{SO}$ and $\mathcal{Z} = Z/\lambda$, we arrive at the main results in Eq. (3).

1. Neto, A. H. C., Guinea, F. N., Peres, M. R., Novoselov, K. S. & Geim, A. K. The electronic properties of graphene. *Rev. Mod. Phys.* **81**, 109–162 (2009).
2. Novoselov, K. S. *et al.* Two-dimensional gas of massless Dirac fermions in graphene. *Nature* **438**, 197–200 (2005).
3. Klein, O. Die reflexion von elektronen an einem potentialsprung nach der relativistischen dynamik von Dirac. *Z. Phys.* **53**, 157 (1929).
4. Katsnelson, M. I., Novoselov, K. S. & Geim, A. K. Chiral tunnelling and the Klein paradox in graphene. *Nature Phys.* **2**, 620–625 (2006).
5. Stander, N., Huard, B. & Goldhaber-Gordon, D. Evidence for Klein tunneling in graphene *p-n* junctions. *Phys. Rev. Lett.* **102**, 026807 (2009).
6. Young, A. F. & Kim, P. Quantum interference and Klein tunnelling in graphene. *Nature Phys.* **5**, 222–226 (2009).
7. Bai, C. & Zhang, X. Klein paradox and resonant tunneling in a graphene superlattice. *Phys. Rev. B* **76**, 075430 (2007).
8. Kumar, S. B. & Guo, J. Chiral tunneling in trilayer graphene. *Appl. Phys. Lett.* **100**, 163102 (2012).
9. Liu, M.-H., Bundesmann, J. & Richter, K. Spin-dependent Klein tunneling in graphene: Role of Rashba spin-orbit coupling. *Phys. Rev. B* **85**, 085406 (2012).
10. Trambly de Laissardiere, G., Mayou, D. & Magaud, L. Localization of Dirac electrons in rotated graphene bilayers. *Nano Lett.* **10**, 804–808 (2010).
11. Park, S. & Sim, H.-S. Klein tunneling and Berry phase π in bilayer graphene with a band gap. *Phys. Rev. B* **84**, 235432 (2011).
12. MacDonald, A. H., Jung, J. & Zhang, F. Pseudospin order in monolayer, bilayer and double layer graphene. *Phys. Scr.* **T146**, 014012 (2012).
13. Bychkov, Y. A. & Rashba, E. I. Properties of a 2D electron gas with lifted spectral degeneracy. *JETP Lett.* **39**, 78 (1984).

14. Nitta, J., Akazaki, T. & Takayanagi, H. Gate control of spin-orbit interaction in an inverted $In_{0.53}Ga_{0.47}As/In_{0.52}Al_{0.48}As$ heterostructure. *Phys. Rev. Lett.* **78**, 7, 1335–1338 (1997).
15. Grundler, D. Large Rashba splitting in InAs quantum wells due to electron wave function penetration into the barrier layers. *Phys. Rev. Lett.* **84**, 26, 6074–6077 (2000).
16. Zhang, X. Negative refraction of spintronics and spin beam splitter. *Appl. Phys. Lett.* **88**, 052114 (2006).
17. Lv, B. & Ma, Z. Electronic equivalence of optical negative refraction and retroreflection in the two-dimensional systems with inhomogeneous spin-orbit couplings. *Phys. Rev. B* **87**, 045305 (2013).
18. Cheianov, V. V., Fal'ko, V. & Altshuler, B. L. The focusing of electron flow and a Veselago lens in graphene *p-n* junctions. *Science* **315**, 5816, 1252–1255 (2007).
19. Peterfalvi, C. G., Oroszlany, L., Lambert, C. J. & Cserti, C. Intraband electron focusing in bilayer graphene. *New J. Phys.* **14**, 063028 (2012).
20. Hassler, F., Akhmerov, A. R. & Beenakker, C. W. J. Flat-lens focusing of electrons on the surface of a topological insulator. *Phys. Rev. B* **82**, 125423 (2010).
21. Berry, M. V. Quantal phase factors accompanying adiabatic changes. *Proc. R. Soc. Lond. A* **392**, 1802, 45–57 (1984).
22. Ando, T., Nakanishi, T. & Saito, R. Berry's phase and absence of back scattering in carbon nanotubes. *J. Phys. Soc. Jpn.* **67**, 8, 2857–2862 (1998).
23. Miktik, G. P. & Sharlai, Y. V. The Berry phase in graphene and graphite multilayers. *Fiz. Nizk. Temp.* **34**, 1012–1019 (2008).
24. Shen, S.-Q. Spin Hall effect and Berry phase in two-dimensional electron gas. *Phys. Rev. B* **70**, 081311 (R) (2004).
25. Ferry, D. K. & Goodnick, S. M. *Transport in Nanostructures. Cambridge Studies in Semiconductor Physics and Microelectronic Engineering*: **6**. Cambridge University Press (1999).
26. Ando, T., Fowler, A. B. & Stern, F. Electronic properties of two-dimensional systems. *Rev. Mod. Phys.* **54**, 2, 437–672 (1982).
27. Schierholz, C., Matsuyama, T., Merkt, U. & Meier, G. Weak localization and spin splitting in inversion layers on *p*-type InAs. *Phys. Rev. B* **70**, 233311 (2004).
28. Ishizaka, K. *et al*. Giant Rashba-type spin splitting in bulk BiTeI. *Nature Mater.* **10**, 521–526 (2011).
29. Ast, C. R. *et al*. Giant spin splitting through surface alloying. *Phys. Rev. Lett.* **98**, 186807 (2007).

Acknowledgments

The project is supported by the Australian Research Council(DP130102956), the NNSFC Grants (91021017, 11274013) and NBRP of China (2012CB921300).

Author contributions

Y.S.A., Z.M. and C.Z. initiated the idea and performed the analysis. Y.S.A. performed the numerical calculation. All authors co-wrote and revised the manuscript.

Additional information

Competing financial interests: The authors declare no competing financial interests.

How to cite this article: Ang, Y.S., Ma, Z.S. & Zhang, C. Chiral-like tunneling of electrons in two-dimensional semiconductors with Rashba spin-orbit coupling. *Sci. Rep.* **4**, 3780; DOI:10.1038/srep03780 (2014).